

THE INVESTIGATION OF POLYMER TEMPLATES BY AFM AND GISAXS

DESY SUMMER STUDENT PROGRAMME 2009

Shestakov Mikhail

Lomonosov Moscow State University

10th September 2009

Contents

<u>1. INTRODUCTION.....</u>	<u>3</u>
1.1 AIM OF THE PROJECT	3
1.2 FUNDAMENTALS OF EXPERIMENTAL TECHNIQUES.....	3
1.2.1 ATOMIC FORCE MICROSCOPY (AFM)	3
1.2.2 GRAZING INCIDENCE SMALL ANGLE X-RAY SCATTERING ANALYSIS (GISAXS)	5
<u>2 EXPERIMENTAL SETUP.....</u>	<u>7</u>
2.1 ATOMIC FORCE MICROSCOPY	7
2.2 GISAXS	7
<u>3 RESULTS AND DISCUSSION.....</u>	<u>8</u>
3.1 AFM	8
3.2 GISAXS	9
<u>REFERENCES.....</u>	<u>13</u>

1. Introduction

1.1 Aim of the project

The aim of this project was to characterize nanostructured polymer templates via atomic force microscopy and to investigate deposited polymer templates by Grazing Incidence Small Angle X-ray Scattering analysis (GISAXS). The group in which I worked during the summer student program used PS-PMMA copolymer templates with a hexagonal arrangement of upright cylinders and samples with a lamellar surface morphology as a template to create highly ordered FePt nanostructures. FePt was in this case deposited via MBE (molecular beam epitaxy) onto the templates which I had to characterize.

1.2 Fundamentals of experimental techniques

1.2.1 Atomic Force Microscopy (AFM)

The atomic force microscope (AFM) is a very high-resolution type of scanning probe microscopy, with demonstrated resolution of fractions of a nanometer, more than 1000 times better than the optical diffraction limit. The precursor to the AFM, the scanning tunneling microscope, was developed by Gerd Binnig and Heinrich Rohrer in the early 1980s, a development that earned them the Nobel Prize for Physics in 1986. Binnig, Quate and Gerber invented the first AFM in 1986. The AFM is one of the foremost tools for imaging, measuring and manipulating matter at the nanoscale. The AFM consists of a cantilever with a sharp tip (probe) at its end that is used to scan the specimen surface. The cantilever is typically silicon or silicon nitride with a tip radius of curvature

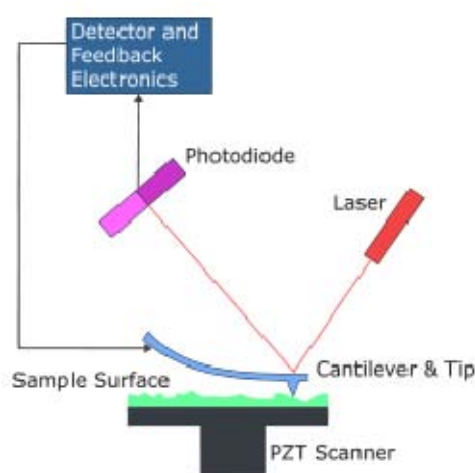


Figure 1. The scheme of atomic force microscope

on the order of nanometers. When the tip is brought into proximity of a sample surface, forces between the tip and the sample lead to a deflection of the cantilever according to Hooke's law. Depending on the situation, forces that are measured in AFM include mechanical contact force, van der Waals forces, capillary forces, chemical bonding, electrostatic forces, magnetic forces (see magnetic force microscope, MFM), Casimir forces, solvation forces, etc. As well as force, additional quantities may simultaneously be measured through the use of specialised types of probe. Typically, the deflection is measured using a laser spot reflected from the top surface of the cantilever into an array of photodiodes. Other methods that are used include optical interferometry, capacitive sensing or piezoresistive AFM cantilevers. These cantilevers are fabricated with piezoresistive elements that act as a strain gauge. Using a Wheatstone bridge, strain in the AFM cantilever due to deflection can be measured, but this method is not as sensitive as laser deflection or interferometry.

If the tip was scanned at a constant height, a risk would exist that the tip collides with the surface, causing damage. Hence, in most cases a feedback mechanism is employed to adjust the tip-to-sample distance to maintain a constant force between the tip and the sample. Traditionally, the sample is mounted on a piezoelectric tube that can move the sample in the z direction for maintaining a constant force, and the x and y directions for scanning the sample. Alternatively a 'tripod' configuration of three piezo crystals may be employed, with each responsible for scanning in the x,y and z directions. This eliminates some of the distortion effects seen with a tube scanner. In newer designs, the tip is mounted on a vertical piezo scanner while the sample is being scanned in X and Y using another piezo block. The resulting map of the area $s = f(x,y)$ represents the topography of the sample.

The AFM can be operated in a number of modes, depending on the application. In general, possible imaging modes are divided into static (also called contact)

modes and a variety of dynamic (or non-contact) modes where the cantilever is vibrated.

1.2.2 Grazing Incidence Small Angle X-ray Scattering analysis (GISAXS)

Up to fifteen years ago, the scattering techniques were limited to three dimensional samples as the strong penetration depth of the radiations and the low signal to noise ratio hampered the surface sensitivity. Quite recently, thanks to the increasingly use of synchrotron radiation, these techniques were extended to surface geometry using the phenomenon of total external reflection of X-rays in the grazing incidence range. The diffraction used in surface science allows to get accurate information on reconstruction of surfaces surface relaxation, buckling and on the atomic position thanks to the precise measurements of crystal truncation rods (CTR). Epitaxies, relaxation of stress, absorption sites and even maps of strains in real space can be obtained for deposit on a surface. In this respect, the field of semiconductors and thin films growth brought a need of knowledge about layer structure and morphology and sizes of quantum dots, supported islands or buried particles which has pushed towards the development of Grazing Incidence Small Angle X-Ray Scattering (GISAXS).

In a grazing incidence experiment, a monochromatic X-rays beam of wavevector \mathbf{k}_i (wavelength λ - wave number $k_0 = [(2\pi)/(\lambda)]$) is sent onto a surface under an incident angle α_i in the range of a few tenth of a degree. Possibly, the in-plane direction of the incident beam $2\theta_i$ is different from zero. The reference cartesian frame is defined by its origin on the surface, its z-axis pointing upwards, its x-axis perpendicular to the detector plane and its y-axis along it. The X-ray beam is scattered along \mathbf{k}_f in the direction $(2\theta_f, \alpha_f)$ by any type of roughness or electronic contrast variation, on the surface or under surface. Because of energy conservation, the scattering wave vector \mathbf{q} defined by:

$$\mathbf{q} = \frac{2\pi}{\lambda} \begin{pmatrix} \cos(\alpha_f)\cos(2\theta_f) - \cos(\alpha_i)\cos(2\theta_i) \\ \cos(\alpha_f)\sin(2\theta_f) - \cos(\alpha_i)\sin(2\theta_i) \\ \sin(\alpha_f) + \sin(\alpha_i) \end{pmatrix}$$

is the central quantity in the scattering process.

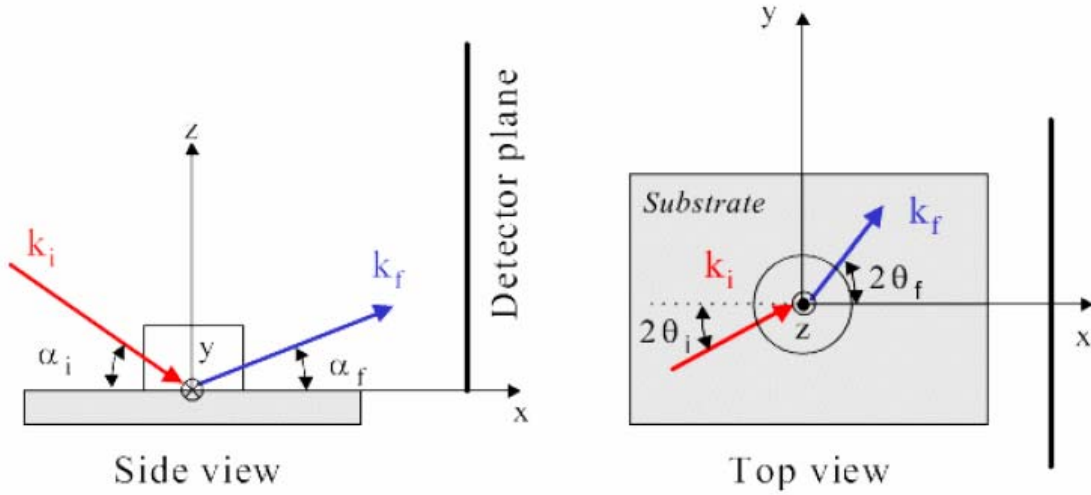


Figure 2. The grazing incidence geometry: an incident wave of wavevector \mathbf{k}_i is scattered in the direction \mathbf{k}_f .

The scattering intensity is recorded on a plane ensuring that the angles are in the few degrees range and thus enabling the study of lateral sizes of a few nanometers. The detector can be punctual (0D), linear (1D) or even bidimensional (2D). The direct beam is often suppressed by a beam stop to avoid the detector saturation as several orders of magnitude in intensity separate the diffuse scattering from the specular reflectivity.

2 Experimental setup

2.1 Atomic Force Microscopy

The AFM measurements were carried out at NT-MDT INTEGRA AURA. We used the non-contact tapping mode to measure the height profile. All measurements were carried out at room temperature.

2.2 GISAXS

The GISAXS measurements were carried out at the beamline BW4 of HASYLAB. The layout of the BW4 beamline is as follows:

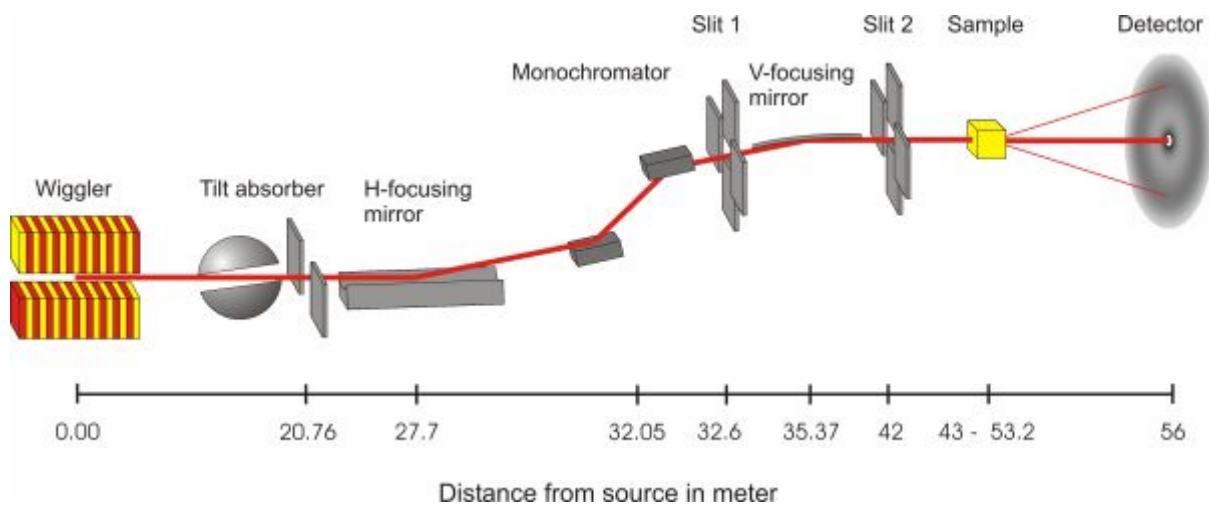


Figure 3. Experimental setup at BW4

The wavelength used was 0.13 nm and a sample-to-detector distance 2 m with an angle of incidence $\alpha_i = 0.8^\circ$. The detector was MarCCD 165 mm in diameter. The exposure time was 60 seconds. The beam size was 30 μm x 60 μm onto the sample.

3 Results and Discussion

3.1 AFM

In the beginning of my project I characterized PS-PMMA copolymer templates with a lamellar surface morphology via AFM. I was asked not to show the pictures here because they were part of a new project. Instead I will focus on the templates with a hexagonal arrangement of upright cylinders. The AFM image of the pure polymer template with a thickness of 90 nm is given in Fig. 4. After depositing the template with FePt at elevated temperatures the surface morphology completely changed into a highly ordered lamellar structure (see Fig. 5). AFM pictures reveal the microscopic surface morphology but they can hardly give information about the arrangement of the deposited FePt. Or in other words, the question I was asked was where is the FePt collected on the template and how does the internal morphology change due to deposition at elevated temperatures? To investigate this GISAXS measurements were taken on these samples.

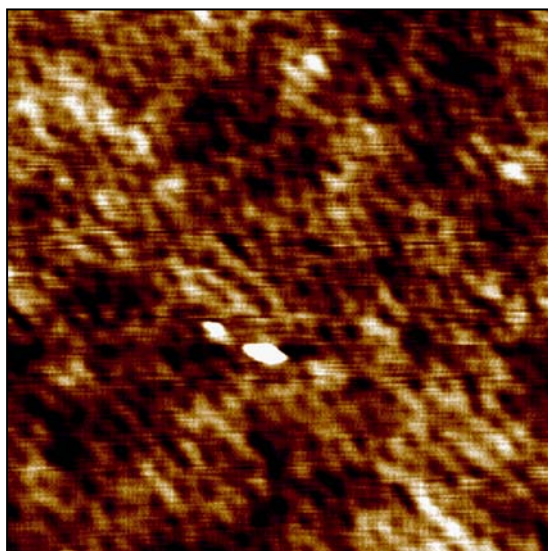


Figure 4. AFM height picture of the virgin PS-PMMA polymer template. The sample consists of an array of upright PMMA cylinders embedded in a PS matrix. The PMMA cylinders were partially removed by treatment of glacial acetic acid. Scan area 1 μm x 1 μm .

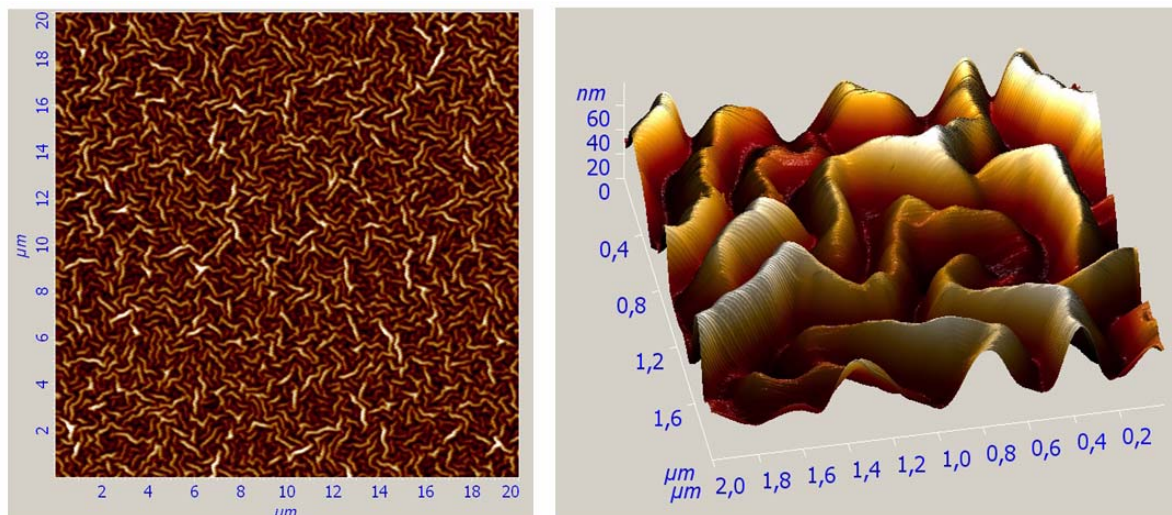


Figure 5. AFM height images of the polymer templates after nominal MBE deposition of 7 nm of FePt at elevated temperature. A drastic change of the surface morphology from a hexagonal arrangement to a highly ordered, canted lamellar structure can be seen. The AFM images don't allow to determine where the magnetic material is deposited. GISAXS investigations were made to clarify this question.

3.2 GISAXS

The GISAXS pictures of the deposited polymer templates were taken at the Hasylab DORIS beamline BW4 and are given in Fig. 6. A drastic change between the two deposition stages of 7 nm and 20 nm can be seen. In the early stage of growth the 2D-GISAXS data set is characterized by horizontal intensity lines which are periodically distributed in the vertical direction. This shows that the FePt nanostructure is placed on a remaining polymer film which creates the GISAXS intensity due to a strongly correlated rough layer of similar thickness. With increasing deposition the scattering intensity becomes less sensitive to the buried polymer film and the fringes get strongly reduced. Instead in the vertical direction additional maxima appear which are typical for a deposited film with small thickness variation. But the most interesting feature can be seen around the specular reflection. Here a hexagonal arrangement of circular intensity maxima can be seen (Fig. 7). The data evaluation was made with the software IsGISAXS [1]. After several days of simulation a lateral arrangement of capped anisotropic pyramids placed on a polymer layer was found which could be used

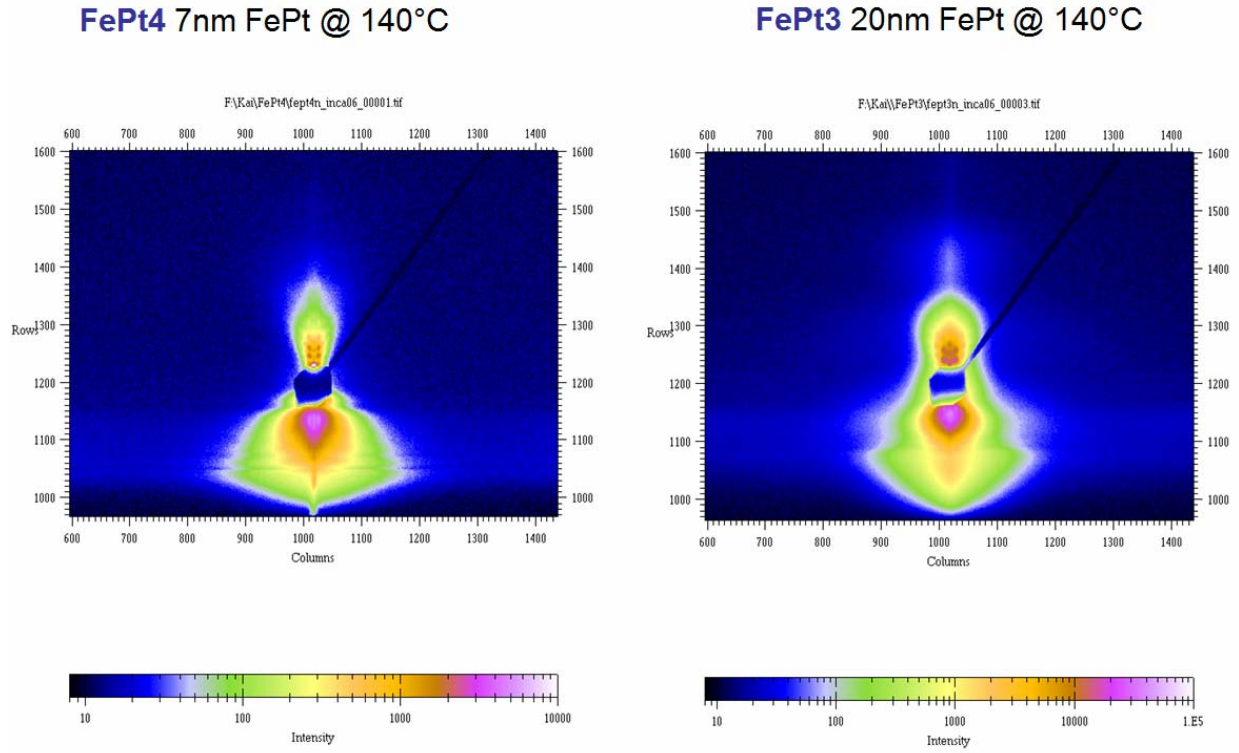


Figure 6. GISAXS images of the polymer templates after nominal deposition of 7 nm and 20 nm of FePt. The exposure time at BW4 was around 60s for each picture.

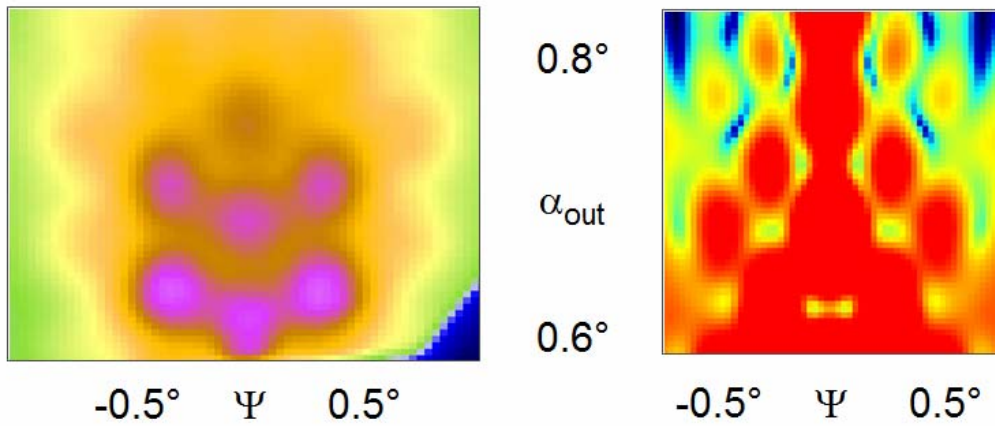


Figure 7. Central region of the GISAXS data (7 nm FePt) slightly above the specular reflection. The right image shows the simulation with the best agreement.

to reproduce the GISAXS structure around the specular reflection with some kind of significance (see Fig. 7). I like to point out that the speed of the simulation was really slow and a better computer would have probably allowed

for even better simulations. The simulation of a 2D picture with low resolution and only a few parameters chosen with distribution took already more than one hour. The parameters for the simulation are given in Fig. 9. The simulation shows that a homogenous FePt is deposited on the anisotropic pyramid structure. The thickness is reduced by 35% compared to the nominal thickness of deposited material. This effect is obviously due to the increased surface area of the nanostructured polymer film compared to a flat film. However, the results indicate that the drastic change of the polymer structure from the hexagonal arrangement to the pyramid like lamellar surface morphology is finished before the FePt MBE deposition started. Thus, this effect is probably due to a thermal treatment before the actual deposition.

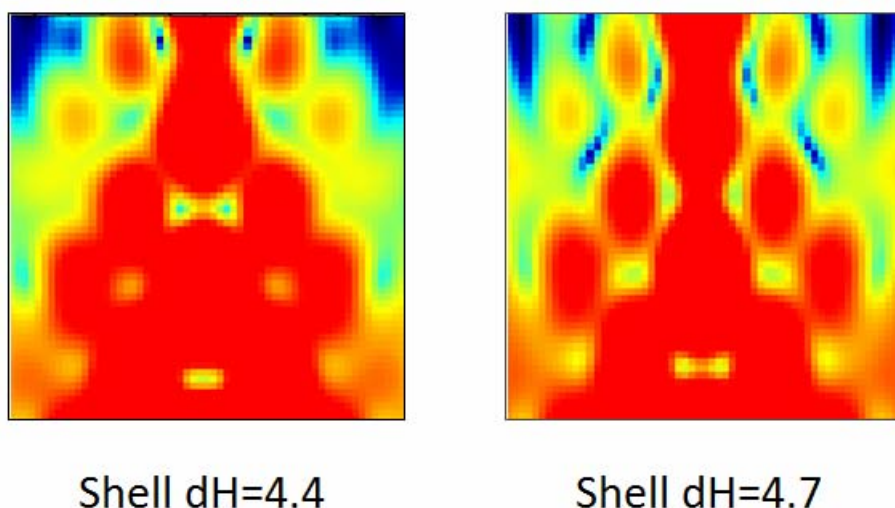


Figure 8. 50% of my time during this summer student project I studied the influence of the variation of structural parameters onto the GISAXS pattern. The goal was to reproduce the experimental data with high significance. Here the thickness of the FePt shell was changed in height and shows a significant change of the GISAXS intensity distribution mainly in the vertical direction.

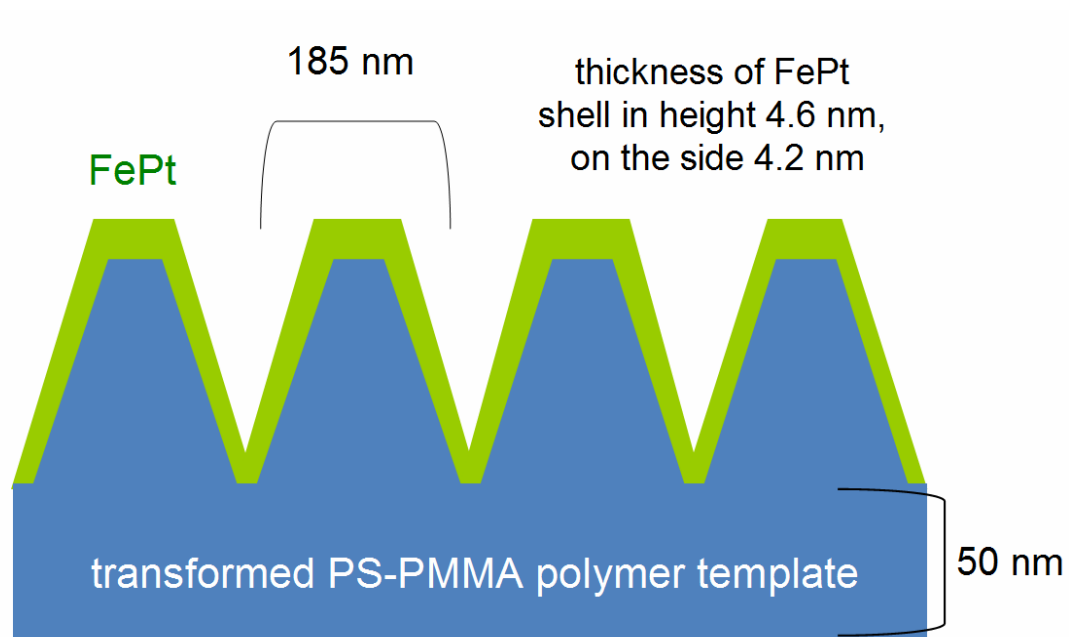


Figure 9. Sketch of selected results extracted from the 2D GISAXS simulation. The evaluation shows that the polymer template transforms into an anisotropic polymer pyramid structure on a polymer film on which the FePt formed a homogenous film of slightly reduced thickness compared to the nominal FePt deposition (7nm). This is probably due to the surface area which is increased compared to that of a flat film due to the 3D morphology. The simulation indicates that the surface morphology of the polymer template was completely transformed into the pyramid like lamellar structure before the FePt deposition started. This interesting transformation is thus an effect caused to thermal radiation and should be further investigated.

References

1. R. Lazzari, F. Leroy, and G. Renaud// Grazing incidence small angle x-ray scattering from islands on surfaces // Phys. Rev. B, 2006.
2. E. Metwalli, S. Couet, K. Schlage, R. Röhlberger et al // In situ GISAXS investigation of gold sputtering onto a polymer template // Langmuir accepted (2007)
3. P. Siffalovic, E. Majkova, L.Chitu, M. Jergel et al // Self-assembly of iron oxide nanoparticles studied by time-resolved grazing incidence small angle X-ray scattering // Phys. Rev. B 76, 195432 (2007)
4. M. M. Abul Kashem, J. Perlich, L. Schulz et al// Maghemite Nanoparticles on Supported Diblock Copolymer Nanostructures// Macromolecules 40, 5075-5083 (2007)